JOURNAL OF AIRCRAFT
Vol. 36, No. 1, January–February 1999

Multidisciplinary Design and Prototype Development of a Micro Air Vehicle

Masoud Rais-Rohani* and George R. Hicks†
Mississippi State University, Mississippi State, Mississippi 39762

This paper discusses the application of multidisciplinary design optimization (MDO) methodology for the design of a very small remotely piloted airplane for a short-range reconnaissance mission. Low Reynolds number aerodynamics and size requirements are used as primary drivers in the conceptual design of the vehicle, and are combined with performance, stability, propulsion, and weight constraints in the design optimization problem. With vehicle size as the objective function, the constrained optimization problem is solved using a penalty function method. Following the analytical validation of the MDO-based design, a prototype of the design vehicle was developed and flight tested. The results of this investigation show that MDO methodology could be used as an enabling technology in creating nonconventional designs that aim at pushing the limits of flight in low Reynolds number regime. They also show that the level of technology incorporated in the propulsion, navigation and communication, and control systems plays a key role in determining the size and weight of micro air vehicles.

Nomenclature

C_D = drag coefficient
C_L = lift coefficient
$C_{L\alpha}$ = lift-curve slope
C_l = rolling-moment coefficient
$C_{l\beta}$ = $\partial C_l/\partial\beta$
$C_{m^{CG}}$ = pitching-moment coefficient about the airplane center of gravity
$C_{m\alpha}$ = $\partial Cm/\partial\alpha$
C_{m0} = pitching-moment coefficient at zero angle of attack
C_n = yawing-moment coefficient
$C_{n\beta}$ = $\partial C_n/\partial\beta$
f = objective function
g = inequality design constraint
M = number of design constraints
N = number of design variables
SM = longitudinal static stability margin
$\boldsymbol{X}$ = vector of design variables
α = angle of attack
β = sideslip angle
δ_e = elevator angle
ε = downwash angle
ε_α = $\partial\varepsilon/\partial\alpha$

Subscripts
b = biplane
i = design variable number
j = design constraint number
m = monoplane

Superscripts
l = lower bound
u = upper bound

Received June 17, 1997; revision received Feb. 17, 1998; accepted for publication Aug. 25, 1998.

*Associate Professor, Department of Aerospace Engineering. Senior Member AIAA.

†Graduate Research Assistant; currently at Sino Swearingen Aircraft Company, 1770 Sky Place Boulevard, San Antonio, TX 78216. Member AIAA.

Introduction

DURING the past several years there has been a growing interest in the design and development of very small aircraft that are generally referred to as micro air vehicles (MAVs). Although the military has been the strongest advocate of this technology,[1] its potential applications go far beyond the battlefields of tomorrow. MAVs are considered to be efficient and inexpensive tools for collecting information in dangerous and hostile environments. For instance, equipped with a sensory device, they could be used for detection of poisonous gases in an environmental disaster area or, if equipped with a video camera, they could be used for various missions of interest to the military, such as reconnaissance, surveillance, targeting, etc. Regardless of their potential applications, the focus is primarily on reducing, as much as possible, the size of such vehicles. The Defense Advanced Research Projects Agency is currently supporting design and development efforts of MAVs that are merely 6 in. across, and capable of performing a mission useful to the military at an affordable cost.[2]

To have a perspective on what it means to have a flying object that is only 6 in. across, let us take a look at nature for a frame of reference. In nature we find birds with wing loading in the range of 0.42–3.56 lb/ft^2 that fly at an approximate sea-level Reynolds number in the range of 7.2×10^3 to 4.12×10^4. The smallest values correspond to a black-chinned hummingbird, and the largest to a mute swan.[3] If we search for a bird with roughly a 6-in. wingspan, we find the winter wren[3] that weighs 0.34 oz with wing loading of 0.48 lb/ft^2 and a cruise speed of 25.6 ft/s (17.5 mph), that flies at an approximate sea-level Reynolds number of 1.37×10^3. Of course, birds have a much more efficient propulsion system than aircraft, and their missions and flight envelopes are not as rigidly defined as those for airplanes; nonetheless, such data give us some idea about the wing loading and operating Reynolds number for a particular size bird or airplane.

What differentiates MAVs from ordinary radio-controlled model aircraft are mainly the small size and flight operation, mostly beyond the visual range of the operator, in very low Reynolds number regimes. The aerodynamics of low Reynolds number flight poses a major challenge in terms of adequate lift generation as well as stability and control requirements. These considerations are the impetus for the renewed interests in flapping wing designs for MAVs as attractive alternatives to fixed wing or rotating wing configurations. One such example is the

ongoing research on insect-like MAVs, referred to as entomopters.[4]

The demand for very small and lightweight MAVs requires miniaturization of flight enabling systems such as the propulsion, control servos, communication and navigation, etc. The propulsion system, in particular, must be compact, lightweight, and highly efficient to provide the MAVs with meaningful range and endurance capabilities. Onboard electronics would also have to be very compact and lightweight with a highly efficient power supply.

To meet the size and weight requirements, MAVs would have to rely on highly integrated systems with multifunctional components. Furthermore, any synergism that may exist among various disciplines would have to be fully exploited to achieve optimal designs for such complex systems. Therefore, MAVs are excellent candidates for the application of multidisciplinary design optimization (MDO) methodology.

In this paper we discuss the application of MDO methodology to the design of a remotely piloted MAV for a short-range reconnaissance mission. We also discuss the analytical validation of the MDO-based design as well as the development and flight testing of a prototype MAV that in shape and size was very close to the predicted design.

Because we intended to build and flight test our MAV design, we used affordable off-the-shelf technologies for the propulsion, control, navigation, communication, and material systems. Therefore, a large portion of the gross weight, including the payload, was already determined.

Mission Requirements

For a given level of technology, the mission, performance, and payload requirements mostly dictate the size and shape of the flight vehicle. For our design we selected the reconnaissance mission as specified by the International Society of Structural and Multidisciplinary Optimization in a recent MAV competition.‡

The mission requires the vehicle to fly a distance of approximately 2000 ft from the launch site to capture a clear image of a 5-ft-size target on the ground, and to deliver that image to the launch site in less than 45 min. The mission profile is depicted in Fig. 1. As the pilot remotely flies the MAV to the vicinity of the target, he makes several shallow dive and climb passes to view and transmit a clear image of the target before heading back to the launch site for landing. Although the target is in the line of sight from the launch site, it is too far away for the pilot to have uninterrupted visual contact with the vehicle. Therefore, an onboard remote sensing device is necessary.

Conceptual Design

As a precursor to the conceptual design, a search was conducted to collect data on wing loading and Reynolds number range on more than 50 small-scale airplanes. We found the Reynolds number for these airplanes to be in the range of 5×10^4 to 8×10^5, corresponding to the wing loading of $\sim 0.5-2$ lb/ft^2. Closer examination revealed that to fly below the Reynolds number of 2×10^5, an average wing loading of about 1.125 lb/ft^2 would be a reasonable value.

We also examined airfoil shapes designed specifically for small airplanes flying in the Reynolds number range of 6×10^4 to 2.5×10^5. We chose the Selig S-3021-095-84 airfoil,[5] based on its drag polar and lift-curve characteristics at relatively low values of Reynolds number. The drag polar for this airfoil indicates a fairly constant drag coefficient over a wide range of lift coefficient. It also shows no laminar bubbles around the Reynolds number of 1×10^5, which is the expected stall value for the MAV design considered here. The Selig airfoil also has a fairly high maximum lift coefficient and a fairly low pitching moment coefficient, both of which would be advantageous in this design.

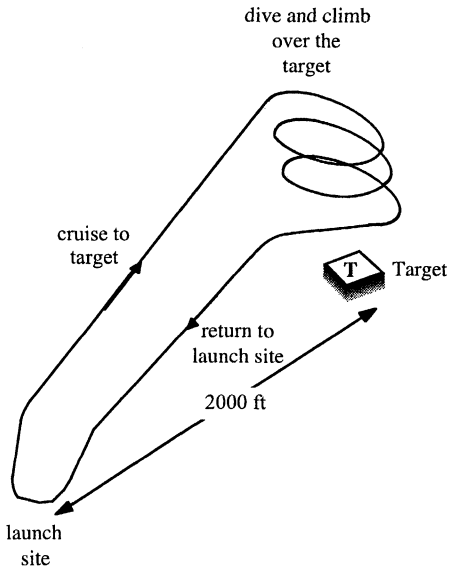

Fig. 1 Reconnaissance mission profile.

With vehicle size, defined as the longest linear distance between any two points on the vehicle, as the main design driver, the wingspan needs to be shortened while maintaining a sufficiently large wing area to keep the wing loading in the desired range. The shortening of wingspan is normally accompanied by an increase in induced drag. However, this adverse effect could be significantly reduced by using a nonplanar wing configuration such as a biplane.

Theoretically, a biplane produces half the induced drag of a monoplane of the same span, or it could be said that for the same amount of induced drag, the biplane produces twice the lift of a monoplane of the same span.[6] This theoretical advantage, however, could only be achieved by spacing the two wings far enough apart to minimize the mutual interference, and it should be balanced against the increase in viscous drag as a result of the doubling of the wetted area of the wing. The biplane configuration is also more efficient structurally in terms of bending stiffness than a monoplane of equal area, and it would allow for low-speed flight during takeoff and landing without the use of high-lift devices.[7]

To quantify the differences in the aerodynamic characteristics of the planar and nonplanar configurations, we calculated lift and drag for a monoplane, a biplane, and a box-wing configuration. The biplane and box-wing configurations are simply constructed by placing two identical monoplane planforms in parallel, one atop the other, which in the case of the box wing, the upper and lower wing tips are joined by flat panels. To equally compare each planform, the configuration was nondimensionalized by the total lifting area of respective planform. A vortex–lattice model was used to calculate the induced drag coefficient. The viscous drag was estimated by integrating an empirical skin friction coefficient, which is based on the local Reynolds number and specified transition value, over the entire wetted area of the wing. The plots of linearized drag polar and lift curve are shown in Figs. 2 and 3 for an angle of attack ranging from 0 to 10 deg. For these plots, the gap-to-span ratio for the biplane and the box wing is set at 50%.

As evident in Fig. 2, the monoplane is found to have the lowest drag among the three configurations for $C_L^2 < 0.19$. However, for greater values of C_L^2, the advantage shifts toward the nonplanar configurations. It is also evident from Fig. 2 that the advantage of the box wing over the biplane could only be realized for $C_L^2 > 0.7$, which is not easily attainable with a low Reynolds number airplane. Therefore, with the expected range

‡"International Society of Structural and Multidisciplinary Optimization's Micro Aerial Vehicle Competition," http://www.aero.ufl.edu~issmo/mav/mav.htm, 1997.

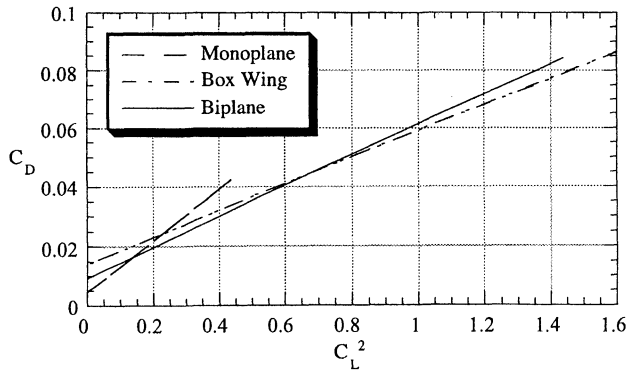

Fig. 2 Linearized drag polar for three different wing configurations. Reprinted with permission, SAE Paper 975547 © 1997.

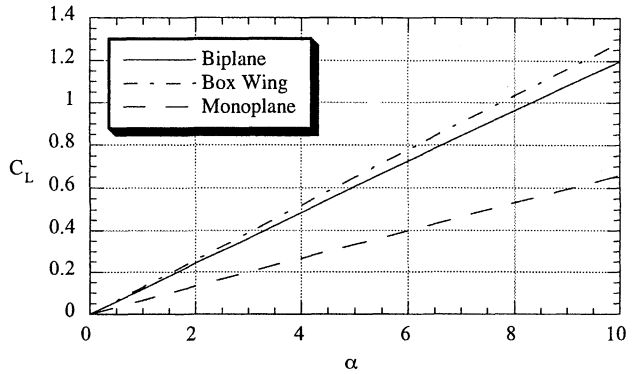

Fig. 3 Lift curve for three different wing configurations. Reprinted with permission, SAE Paper 975547 © 1997.

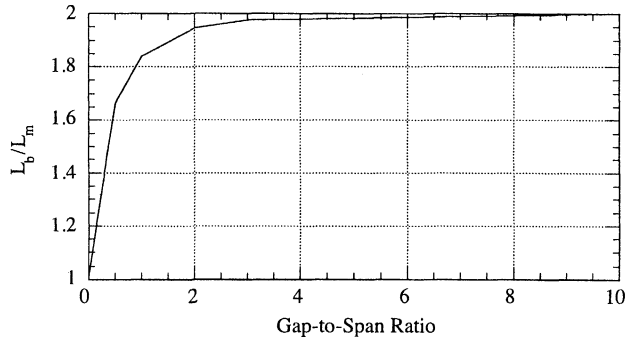

Fig. 4 Effect of gap size on biplane-to-monoplane lift ratio.

of C_L for our MAV design being between 0.48 and 1.1, the biplane would be the most preferred configuration.

Figure 3 shows the nonplanar configurations to have higher $C_{L\alpha}$ than the corresponding monoplane. This is crucial because the onboard camera, that is used to remotely fly the MAV and navigate it to and from the target, is mounted at a fixed position. Therefore, the airplane must stay within a reasonable range of angle of attack, i.e., $\alpha \approx 6.5$ deg, in our case using $C_{L\alpha} = 0.096$/deg, for the pilot to have the necessary situational awareness.

To quantify the effect of gap size on the aerodynamic characteristics of the biplane configuration, one must first examine the possible gains that can be realized. It can be hypothesized that by doubling the monoplane wing area, as in the case of the biplane, twice as much lift can be generated. To examine this hypothesis, we compared the biplane-to-monoplane lift ratio (L_b/L_m) for a range of gap-to-span ratios. Figure 4 indicates that L_b/L_m increases very rapidly up to the gap-to-span ratio of 0.5, and then it increases at a more moderate rate, and soon after, it levels off at the gap-to-span ratio of approximately 3.

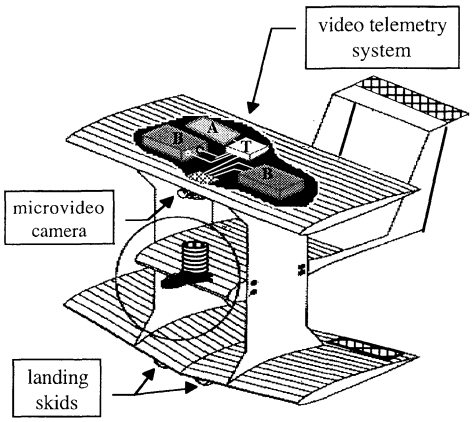

Fig. 5 Isometric view of the conceptual design configuration.

Figure 4 also shows that the doubling of the lift is attainable only for a gap-to-span ratio of around 10, which obviously is not feasible. However, it can be seen that a gap-to-span ratio of around 0.5 results in a 60% increase in the lift. For an MAV, this could translate into a substantial gain in performance. We need to point out also that the gap-to-chord ratio, although important in most cases, does not play any role in our design because there is no change in the maximum lift coefficient of the Selig airfoil over the Reynolds number range of 1×10^5 to 2.5×10^5.

Finally, the presence of dihedral could help improve the lateral stability of the biplane. Consequently, with the lower wing positioned far below the center of gravity of the airplane, it will be allowed to have a positive dihedral.

To keep the airplane size to a minimum, the fuselage length cannot exceed the wingspan. A short fuselage, however, could adversely affect the longitudinal stability as the tail is brought closer to the center of gravity of the airplane. To remedy this problem, a larger-than-normal tail could be used to produce the required pitching moment. In addition, the close proximity of the tail to the wing could pose an aerodynamic problem in terms of downwash. As a result, a high tail configuration is chosen such that it would be slightly above the upper wing in level flight.

Besides the elevator, ailerons are used for directional control. The rudder is eliminated in the design as the MAV is to be hand launched. These control surfaces are operated remotely by microservos attached to a radio-control receiver.

The conceptual design work culminated in the biplane configuration shown in Fig. 5. This computer-aided design (CAD) drawing shows the MAV's layout with limited detail. The upper and lower wings are straight and untapered with the lower wing having a positive dihedral. Both wings are similar in airfoil shape and size. The fuel tank along with the airborne ratio control unit are housed inside the forward fuselage section immediately behind the engine, which is mounted on the nose of the airplane.

Flight Enabling Systems

Remote Sensing and Image Capture System

Among the concepts considered for remote sensing and image capture system, an onboard video telemetry system is found to be most efficient in performing two critical functions: 1) helping the pilot navigate and fly the airplane to the target; and 2) transmitting a clear video image of the target that could be received and recorded at the launch site.

Because the video telemetry system constitutes the payload in our design, it has a strong influence on the gross weight and size of the MAV. Consequently, it is necessary to use a system that can transmit a video signal over a radius of half a mile while at the same time being as lightweight, compact, and affordable as possible. The microvideo technology has been

evolving rapidly, and its components are becoming smaller and lighter every year. However, the cost of these components is still relatively high, and depends highly on their compactness and level of performance.

Based on some tradeoff studies, we decided to use a 0.7-oz black and white in-line microvideo camera, a 2-oz, 2.4-GHz transmitter, an omni-directional antenna, and two 9-V batteries with a combined weight of 2.7 oz to power the camera and transmitter separately. The entire video telemetry system, shown in Fig. 5, weighs approximately 5.6 oz. Although, this weight would be considered very light by most standards, it is still not light enough for future MAV designs, which will end up having gross weight of 3 oz or less.

On the receiving end, the system consists of a 2.4-GHz receiver connected to a flat-plate directional antenna and powered by a 12-V battery. The receiver is connected to a TV that the pilot uses to fly the MAV beyond the normal visual range.

Airframe Material System and Design

In trying to reduce the structural weight, a low-density material of sufficient strength and stiffness must be used. We examined various material systems ranging from lightweight fiber-reinforced plastics to commonly used balsa, and in evaluating the pros and cons of these materials, we selected balsa as the primary material system.[8]

The fuselage is divided into two sections. The fore section has a rib-frame design with an enclosed volume for housing the fuel tank and the airborne radio-control unit. The aft section consists of a dual boom made of truss structures with balsa members. The tail also has a balsa primary structure.

The wings are composed of a built-up main spar positioned near 30% chord with two stringers near 60% chord. Extra support is provided by thin ribs, spaced at regular intervals along the span. The upper and lower wings are attached together with a thin sheet of plywood on each side of the fuselage fore section as shown in Fig. 5. The wings and fuselage are covered by a thin Monokote™ plastic film.

The structural weight of the airplane is calculated based on each component size and estimated quantity and size of individual airframe parts.

Propulsion System

Without a doubt, the propulsion system plays a key role in design and operation of an MAV. It is crucial for the propulsion system to be very efficient, compact, and lightweight. Its efficiency determines how much fuel or electric power must be carried onboard, which combined with its compactness and light weight, can help reduce the size and weight of the MAV.

The two main propulsion systems we considered for our MAV design are 1) internal combustion engines, and 2) electric motors. The internal combustion engines are relatively compact and efficient, and can operate for long duration on standard or chemically enhanced fossil fuel, but the unit and its required fuel are rather heavy. On the other hand, the electric motors are lightweight and compact, but cannot operate for a long time before they drain the power supply. The batteries available on the market to operate these motors are still rather heavy and have a short lifespan. Based on the mission requirements and the options available, we chose the internal-combustion engine.

The information provided by the manufacturers of small internal-combustion engines is usually limited to engine size and horsepower. However, in sizing the airplane, it is necessary to know the thrust, which is a function of engine horsepower as well as propeller efficiency and airspeed. The fuel consumption rate of the engine is also needed to know how much fuel is required to complete the mission. Therefore, because of insufficient engine data, we conducted a series of wind-tunnel tests on four different engine/propeller combinations. We used a computer-based data acquisition system to make accurate measurements of thrust as a function of tunnel dynamic pressure.

The engines tested were Cox .049, Enya 15, O.S. 28F, and O.S. 40FP with 0.049, 0.15, 0.28, and 0.4 in.^{3} of displacement, respectively. Because of the limited scope of this activity we only tested a single propeller with each engine; hence, our experimental results cannot be used for any generalization of the performance of these engines. We also did not examine the effects of propeller efficiency or disk loading on the thrust generated by each engine.

With an engine mounted on the wind-tunnel sting and in the off position, a baseline drag measurement was made. Then, with the engine turned on and running at full throttle setting, the thrust was measured for each incremental increase in the tunnel dynamic pressure, which was then used to extract the airspeed. Figure 6 shows the experimental data for thrust vs airspeed at zero angle of attack for the four engine/propeller combinations tested.

The static thrust of each engine corresponds to the zero airspeed reading in Fig. 6. The smallest engine produced a static thrust of 0.7 lb, whereas the largest engine produced 3.7 lb of static thrust. The data collected indicate that among the four engines tested, Cox .049 has the lowest drop in thrust with increased airspeed. This, however, could be attributed to the higher disk loading of the propeller used with this engine. For the other three engines, thrust remains fairly constant for airspeeds up to about 45 ft/s, then drops gradually for speeds reaching 70 ft/s, and more rapidly beyond 80 ft/s airspeed. This drop is most apparent with the O.S. 28F engine, which is attached to a low-pitch propeller that increases thrust for the lower values, but decreases it for the higher values of airspeed.

The fuel consumption rate was estimated by recording the time each engine took to consume 8 fl oz of fuel at a constant throttle setting. The estimated fuel consumption rates for all engine/propeller combinations are given in Table 1. The specific fuel weight of 8.9 lb/gal was obtained by measuring the weight of a known volume of fuel.

The measured values of engine thrust, fuel consumption rate, and weight are plotted against the cubic displacement in Fig. 7 for all four engines. As the distribution appears to be fairly linear for each case, a linear curve fit is used to determine an empirical equation for each engine parameter as a

Table 1 Estimated fuel consumption rates for the engine/propeller combinations tested

Engine	Fuel consumption rate, gal/h
Cox .049	0.066
Enya 15	0.166
O.S. 28F	0.182
O.S. 40FP	0.358

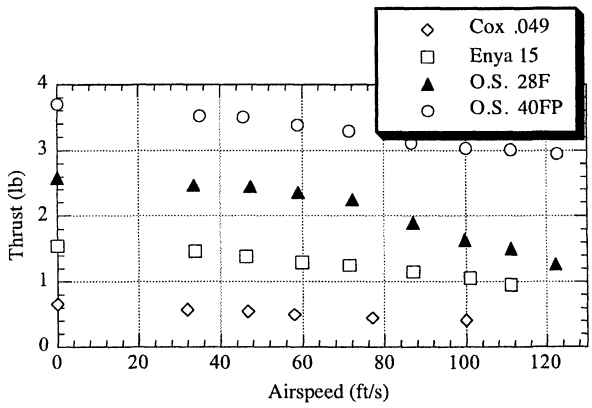

Fig. 6 Wind-tunnel measurements of thrust vs airspeed. Reprinted with permission, SAE Paper 975547 © 1997.

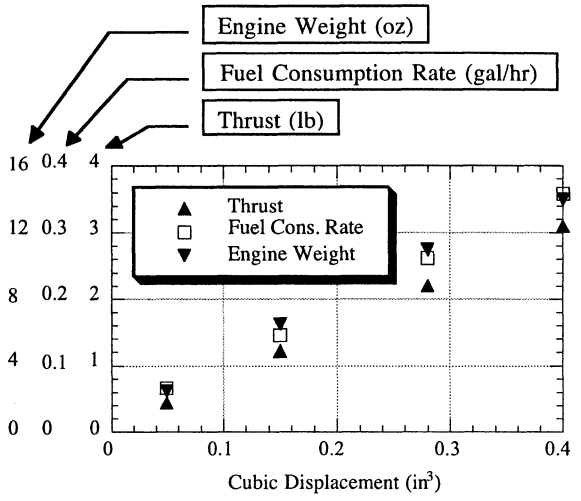

Fig. 7 Engine data as a function of cubic displacement.

function of cubic displacement. Of particular importance is the empirical equation for thrust, which makes it possible to estimate the available thrust for a given-size engine (between 0.05 and 0.4 in.^{3}) at the estimated cruise speed of 80 ft/s or 55 mph.

Multidisciplinary Design Optimization

As mentioned in the Introduction, we use MDO methodology to take advantage of the synergism among various disciplines to achieve an optimal design. The MDO procedure is depicted in Fig. 8. The disciplines considered in the design optimization are aerodynamics, performance, stability, control, and propulsion.

The design optimization problem in Fig. 8 is formulated as

$$\begin{aligned} &\text{Minimizes } f(\boldsymbol{X}) \\ &\text{subject to } g_j(\boldsymbol{X}) \le 0 \qquad \text{for } j = 1 \text{ to } M \\ &\qquad\qquad X_i^l \le X_i \le X_i^u \qquad \text{for } i = 1 \text{ to } N \\ &\text{where } \boldsymbol{X} = (X_1, X_2, \ldots, X_N)^T \end{aligned} \tag{1}$$

The objective function is considered to be the diagonal distance between the opposite tips of the lower and upper wings. A careful examination of the design problem guided by a preliminary analysis led us to the selection of the set of design variables listed next. X_1 = wing chord, X_2 = wingspan, X_3 = horizontal tail span, X_4 = horizontal tail chord, X_5 = distance measured from wing aerodynamic center (a.c.) to tail a.c., X_6 = horizontal tail incidence angle, and X_7 = longitudinal center of gravity location measured from wing leading edge. These variables have a direct influence on the size, weight, aerodynamic performance, and stability characteristics of the MAV. The fuel weight and engine size are noticeably absent in the preceding design variable list. This is because, based on the available data for each engine, we know the amount of fuel an engine needs to operate at full throttle for a period of 10 min, which is thought to be sufficient to perform the specified mission. This fuel weight is then used in the design analysis, and the optimum propulsion system is defined as the smallest-size engine that enables the MAV to perform this mission.

The selected set of design and side constraints are listed next: 1) wing loading $\le$ 1.375 lb/ft^2, 2) thrust-to-weight ratio $\ge$ 0.5, 3) horizontal tail area $\le$ 40% wing area, horizontal tail span $\le$ 50% wingspan, 5) fuselage length $\le$ wingspan, 6) $C_{m0} \ge 0.025$, $C_{ma} \le -0.025$, and 8) gross weight $\le$ 2.55 lb. These constraints are chosen to impose upper bounds on the weight and size of MAV design while simultaneously ensuring adequate performance and stability margins. The limits on stability

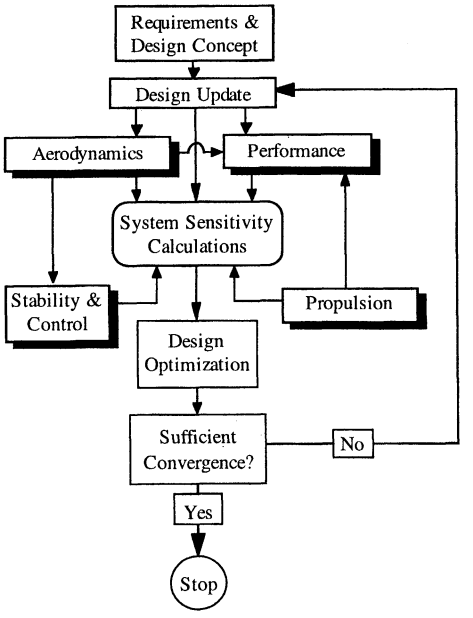

Fig. 8 Flowchart depicting the MDO process.

derivatives are obtained from Ref. 9. The biplane gap-to-span ratio at the fuselage centerline is held constant at 50% and the lower-wing dihedral angle is fixed at 10 deg.

An MDO computer code consisting of separate modules for aerodynamics, propulsion, performance, weights, and optimization was developed in this investigation. The aerodynamics module uses a general nonplanar vortex–lattice program to compute the forces and moments acting on a given airplane configuration. This module also provides output for C_{m0}, $C_{m\alpha}$, $C_{n\beta}$, and $C_{l\beta}$, allowing the examination of lateral and longitudinal static stability margins.

In an effort to reduce the computational burden during the optimization process, a coarse grid was used for the aerodynamic analysis. This made it necessary to analyze the final design very carefully with a finer grid to validate the aerodynamic characteristics of the design.

The propulsion module consists of empirical equations to estimate the thrust, weight, and fuel consumption rate for a specified engine/propeller combination. The performance module contains a collection of closed-form equations for calculations of various performance measures. The weights module contains equations for estimating the structural weight of the airframe from the geometric design variables and the size of structural components made of balsa. The structural weight is added to that of the engine, fuel, payload, and the radio-control system to estimate the gross weight of the MAV. These modules are linked with NEWSUMT-A[10] optimization package for optimization analysis. As shown in Fig. 8, the result of optimization is checked for convergence. If convergence is not reached, the design is updated and the procedure depicted in Fig. 8 is repeated.

Optimization Results

The optimization problem described by Eq. (1) was solved using the extended interior penalty function method. Wherever necessary, the finite difference scheme was used to find the derivatives of constraints with respect to design variables. The optimization problem was solved based on an initial set of the design variables that satisfied all of the constraints. Hence, the search for an optimum design began from inside the feasible design domain.

As stated earlier, the optimization analysis was performed for different-size engines. Among the engine sizes available, the 0.25-in.^{3} engine was the smallest one that could yield an optimum design. It took four optimization cycles, for a total

Table 2 Initial and final values of the design variables based on the O.S. 25FP engine

Design variable definition	Initial values	Final values
Wing chord, in.	9.0	7.98
Wingspan, in.	24.0	20.32
Tail span, in.	8.4	9.00
Tail chord, in.	6.0	6.31
Distance from wing a.c. to tail a.c., in.	16.8	8.76
Tail incidence angle, deg	−1.4	−1.36
Longitudinal location of c.g., in.	1.8	0.025

of 40 one-dimensional minimization iterations, to arrive at an optimum solution using the 0.25-size engine. The values of the initial and final design variables are given in Table 2.

The MDO-based design corresponds to a biplane MAV with a wingspan of approximately 20 in., with an estimated gross weight of 2.54 lb. The design constraints are very close to being active for the final design. The largest constraint margin is 0.430, and the smallest is 0.0025. The final wing loading is 1.13 lb/ft^2, with the structural weight estimated to be 0.78 lb.

The calculation of the desired center of gravity location depends on the accuracy of the moment calculation in the aerodynamic analysis. In this case, the use of a coarse chordwise mesh resulted in a poor estimation of the neutral point location. This issue is addressed in the post-MDO synthesis discussed next.

Post-MDO Synthesis

The aerodynamic and stability characteristics of the final design need to be carefully evaluated to validate the MDO-based solution prior to prototype development. A vortex–lattice program, named SUB3D,[11] is used for the aerodynamic analysis of the design obtained through the MDO procedure. This program provides more accurate aerodynamic data and estimates of the stability derivatives. A much finer grid is used in this case, in part to provide a better estimate for C_m.

The results of this analysis showed that the maximum sectional loading is at the wing root, as would be expected with a straight and rectangular planform. This eliminates the threat of tip stall, which is a big concern for low Reynolds number wings that have a relatively high wing loading. Laminar flow tends to separate easily from the wing, particularly when flying slow, such as in a landing approach. With the wing tailored to stall first at the root, the MAV will not be subjected to the undesired snap rolling tendency that many small airplanes exhibit during landing.

In terms of stability, the concern is primarily with the longitudinal static stability margin because of the biplane configuration coupled with the short tail moment arm. The concern arises from the increase in ε_α, which could become large enough to move the airplane's neutral point ahead of the wing's aerodynamic center. The low-aspect-ratio biplane with a large $C_{L\alpha}$ could amplify this problem. If ε_α ever becomes greater than 1.0, the neutral point will move ahead of the wing's quarter chord, requiring the center of gravity to be pushed ahead of this already far-forward location.

Examination of the final design variable vector in Table 2 indicates that the fuselage length, which is based on the value of design variable 5, is much shorter than the wingspan. It is, therefore, possible to increase the fuselage length to improve the longitudinal stability margin without increasing the *size* of the airplane. The lengthening of the fuselage, however, increases the structural weight of the airplane and could adversely affect the thrust-to-weight ratio constraint imposed during the optimization process. In examining the final design, the thrust-to-weight ratio constraint was found to have the largest margin. Hence, it would be possible to slightly increase the structural weight without suffering a major penalty in the design. Consequently, to have a somewhat higher longitudinal stability margin, the distance of 8.76 in. obtained for design variable 5 was increased to 11.3 in.

Figure 9 shows the variation in $C_{m_{CG}}$ with changes in α. The slope of this curve, i.e., $C_{m\alpha}$, must be negative to ensure longitudinal static stability. Note that at a center of gravity location of 25% mean aerodynamic chord (m.a.c.), MAV design is unstable for $\alpha < -5$ deg and is barely stable for $\alpha > -5$ deg. The other two curves in Fig. 9 show that $C_{m\alpha}$ becomes increasingly more negative as the center of gravity is moved forward.

A benchmark for longitudinal stability is the static margin. In this case, a stick-fixed static margin in the range of 5–8% would be used to allow a reasonable margin of safety when test flying the prototype MAV. The C_L is found to be 0.5 for the airplane cruising at sea level at a speed of 45 mph. Through an iterative solution procedure, we trimmed the MAV for steady-level flight and calculated the stability derivatives $C_{m\alpha}$ and $C_{L\alpha}$. With these derivatives known, we calculated the longitudinal static stability margin as[12]

$$SM = -(C_{m\alpha}/C_{L\alpha})100\% \tag{2}$$

We examined the SM values for three different center of gravity locations, as listed in Table 3, and chose a center of gravity location of 18% m.a.c.

For the pilot to be able to trim the airplane over its flight envelope, adequate elevator area is needed. Because of the limited tail moment arm, we initially chose an elevator size equal to one-half tail area. This size proved to be overly adequate in the aerodynamic analysis, which was done by trimming the airplane at C_L values above and below its operational range to see how much elevator deflection was required. The calculations were done at a forward center of gravity position of 15% m.a.c. because it would require the most control-surface deflection. At $C_L = 1.2$, it was necessary to have $\delta_e = -8.74$ deg to trim the airplane, whereas at $C_L = -1.2$, a $\delta_e = 0.34$ deg was needed for trim. This analysis indicated that the elevator was unbalanced as the required up and down deflections were different.

The plot of $C_{M_{CG}}$ vs δ_e in Fig. 10 shows that, for the current design, the elevator does not cause a nose-down pitching moment until δ_e has reached −5 deg. This problem, however, is remedied by decreasing the tail incidence angle to −2.5 deg,

Table 3 Longitudinal static stability margins for different center of gravity locations

c.g. location, % m.a.c.	SM, %
25	0.602
20	3.129
18	7.649
15	16.360

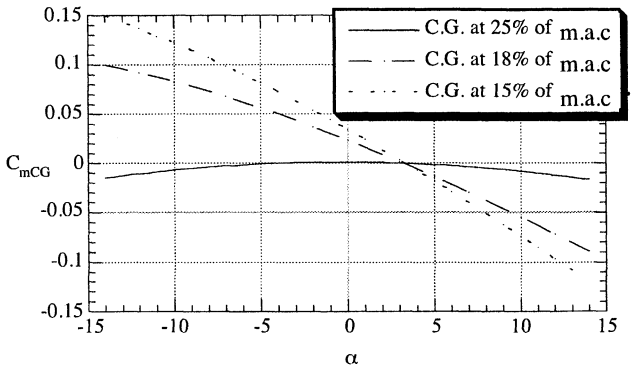

Fig. 9 Variation in pitching moment coefficient with α. Reprinted with permission, SAE Paper 975547 © 1997.

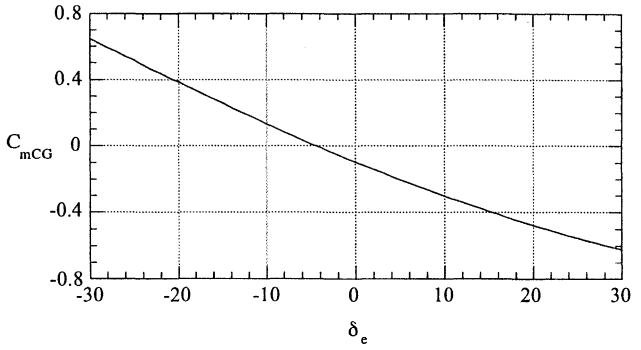

Fig. 10 Variation in pitching moment coefficient with δ_e. Reprinted with permission, SAE Paper 975547 © 1997.

which relaxes the amount of δ_e required to trim the MAV. It should also be noted that the tail efficiency factor for low Reynolds number airplanes is very low because of the thick boundary layers that develop on the wing and fuselage. This is another reason that a large tail surface is needed to provide adequate control.

The final MAV design has $C_{L\alpha}$ = 0.1/deg, which is surprisingly high for such a low-aspect-ratio design, but is consistent with the results found in the preliminary study comparing the biplane and monoplane configurations. Its drag polar also indicated a desirable characteristic with the $C_L|_{\text{cruise}}$ = 0.5 being very close to C_L for minimum drag.

Prototype Development

The construction of the prototype MAV began as the post-MDO synthesis was nearing completion. The size and geometric specifications used to construct the prototype MAV were based on the results of MDO and those modifications that took place as a result of post-MDO synthesis. The prototype's geometric and weight specifications are given next. Geometry: wingspan = 22 in., wing chord = 8 in., lower wing dihedral = 10 deg, gap-to-span ratio at fuselage centerline = 50%, tail incidence angle = −2.5 deg, and tail area = 41.44 in.^{2} Weight (lb): airframe = 1.3, engine = 0.813, video telemetry system = 0.35, radio-control system = 0.3, fuel = 0.28, spinner = 0.25, and gross takeoff = 3.3.

The gross weight of the prototype is about 29% higher than that predicted by the MDO analysis. This is mainly a result of two factors. First, the structural weight estimation was based on a more efficient airframe, whereas the prototype was built somewhat conservatively, resulting in a rather heavy structure. Second, the prototype center of gravity was off target, which required the addition of a heavy spinner (7.6% of gross weight) to bring the center of gravity to a desired forward location. We could not move the engine forward because that would have increased the longitudinal dimension of the MAV. Also, there was a rigid time constraint on the construction and flight testing of the prototype, and consequently, modifications that would have reduced the weight of the MAV could not be implemented. Considering all of these factors, the prototype MAV is in reasonably good agreement with the MDO-based design.

The combined weight of the propulsion, fuel, video telemetry, and radio-control systems constitutes more than 50% of the gross weight of the MAV. This clearly indicates the need for further miniaturization of these systems to substantially reduce the size and weight of future MAVs. Figure 11 shows a photograph of the prototype MAV, which took nearly 120 labor hours to complete and prepare for flight testing.

Flight Testing

Flight testing proceeded shortly after the construction and balancing of the prototype were completed. The MAV was successfully hand launched from a ground vehicle moving at a speed slightly higher than its stall speed of approximately 19 mph. Following the launch, the pilot easily trimmed it for steady level flight and tested it in different maneuvers. The pilot had full control of the MAV at near and far distances, and the controls were very responsive to his commands. A photograph of the prototype MAV in flight is shown in Fig. 12.

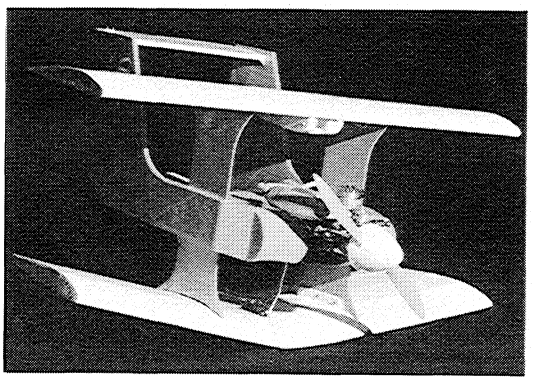

Fig. 11 Prototype MAV. Reprinted with permission, SAE Paper 975547 © 1997.

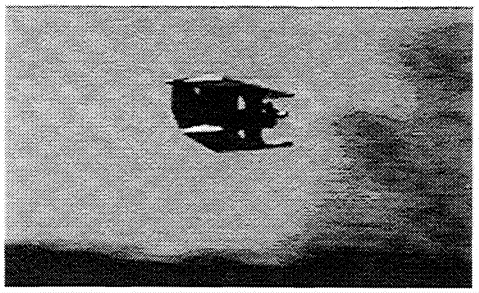

Fig. 12 Prototype MAV in flight. Reprinted with permission, SAE Paper 975547 © 1997.

Both low- and high-speed characteristics of the airplane were evaluated and found to be satisfactory. Despite the close proximity of wing and the tail, the airplane proved to be sufficiently stable with extremely good flying qualities, including gentle stall characteristics. Also, the MAV had no noticeable tendency for control-surface flutter at high speeds. The short wingspan provided the airplane with great agility in lateral motion. The climb performance was also good as a result of a relatively high thrust-to-weight ratio. As expected, in the absence of conventional landing gear, the MAV required a more cautious landing.

The video telemetry system also worked successfully. Although a black and white video camera was used, the aerial picture was very clear with good contrast. The 2.4-GHz receiver at the launch site had no difficulty with the reception of the signal at short and long distances.

Concluding Remarks

The MDO methodology was successfully applied in the design of an MAV for short-range reconnaissance. The desire to reduce the MAV size had to be carefully balanced against aerodynamic efficiency and control stability margins to obtain an optimum design that could perform the specified mission.

The development of the MDO code containing aerodynamics, propulsion, performance, stability and control, weight, and optimization analysis modules in a short time proved to be very challenging. However, its implementation was crucial for obtaining an optimal MAV design.

The results of this study indicate that nonconventional designs should be considered to reduce the size of future MAVs to around 6 in. or potentially even smaller, depending on the specified mission and the level of technology incorporated in

their propulsion, navigation, communication, and control systems.

The prototype development provided a valuable experience and proved the old adage that the weight always tends to increase when the design is manufactured. In our case the prototype was 29% heavier than the MDO-based design. This margin could be reduced substantially, however, if 1) a more accurate model of the airframe is used for weight calculation, and 2) vehicle balance and center of gravity location are not significantly altered during its construction. It is also noteworthy to mention that the flight-enabling systems, i.e., propulsion, video telemetry, and radio control, constituted more than 44% of the gross weight of the prototype MAV. This clearly demonstrates the need for further miniaturization of these systems.

The flight testing of the MAV substantiated many of the assumptions and predicted characteristics of the vehicle in flight. Although the MAV was designed primarily based on its cruise condition, it did have excellent characteristics in all flight modes.

The major drawback of the prototype MAV was in its launch. Because of its relatively heavy weight, it could not be launched from a stationary platform. However, a catapult launch mechanism, such as the one commonly used by the military, could help overcome this problem.

Acknowledgments

We would like to thank the members of Mississippi State University's Micro Aerial Vehicle competition team: Gregory Bartz for constructing the prototype, Andy Ko and Carolyn Dear for their work on the video telemetry system, Michael McNabb for his help with the wind-tunnel tests, and Michael Cancienne and Michael Hazlewood for their help with some of the calculations. All of these undergraduate aerospace engineering students provided assistance with the flight testing of the prototype MAV. The financial support for this work was provided by the Department of Aerospace Engineering at Mississippi State University.

References

[1]"Military Applications of Micro Air Vehicles (MAVs)," User/Developer Workshop, Ft. Huachuca, AZ, Oct. 1996.

[2]"Tactical Technology Solicitations: BAA 97-29 and 97-30," Defense Advanced Research Projects Agency, 1997.

[3]Tennekes, H., *The Simple Science of Flight, from Insects to Jumbo Jets*, MIT Press, Cambridge, MA, 1997.

[4]Stone, A., "Flying into the Future, Miniature Flying Machines Could Help with Warfare, Agriculture and More," Research Horizons, Georgia Inst. of Technology, Atlanta, GA, 1997.

[5]Simons, M., *Model Aircraft Aerodynamics*, 3rd ed., Argus Books, Herts, England, UK, 1994.

[6]Raymer, D. P., *Aircraft Design: A Conceptual Approach*, AIAA Education Series, AIAA, Washington, DC, 1989.

[7]Stinton, D., *The Design of the Airplane*, Reinhold, New York, 1983.

[8]Lennon, A., *The Basics of R/C Model Aircraft Design*, Air Age Inc., Wilton, CT, 1996.

[9]Nelson, R., *Flight Stability and Automatic Control*, McGraw–Hill, New York, 1989.

[10]Grandhi, R. V., Thareja, R., and Haftka, R. T., "NEWSUMT—A: A General Purpose Program for Constrained Optimization Using Constraint Approximations," *Journal of Mechanics, Transmissions, and Automation in Design*, Vol. 107, 1985, pp. 94–99.

[11]Flansburg, B., "SUB 3D for Windows," *User's Guide*, Softwaeronautics, Inc., 1997.

[12]McCormick, B. W., *Aerodynamics Aeronautics and Flight Mechanics*, 2nd ed., Wiley, New York, 1995.